

## Article

# Is Climate or Direct Human Influence Responsible for Discharge Decrease in the Tunisian Merguellil Basin?

Khaoula Khemiri <sup>1,2,\*</sup>, Sihem Jebari <sup>1</sup>, Ronny Berndtsson <sup>3,\*</sup> and Khelifa Maalel <sup>2,4</sup>

<sup>1</sup> National Research Institute for Rural Engineering, Water and Forestry, BP 10, Tunis 1004, Tunisia; sihem.jebari@gmail.com

<sup>2</sup> National Engineering School of Tunis (ENIT), University of Tunis El Manar, BP 37, Tunis 1002, Tunisia; khelifa.maalel@enit.utm.tn

<sup>3</sup> Centre for Advanced Middle Eastern Studies, Lund University, 223 62 Lund, Sweden

<sup>4</sup> Laboratory of Modelling in Hydraulics and Environment (LMHE), BP 37, Tunis 1002, Tunisia

\* Correspondence: khemiri.khaoula@gmail.com (K.K.); ronny.berndtsson@tvrl.lth.se (R.B.); Tel.: +216-50580465 (K.K.); +46-462228986 or +46-462229609 (R.B.)

**Abstract:** Climate change and direct anthropogenic impact are recognized as two major factors affecting catchment runoff. This study investigated the separate effect of each of these factors for runoff from the important Tunisian Merguellil catchment. For this purpose, more than forty years of hydrological data were used. The methodology was based on hydrological characterization, NDVI index to monitor land use dynamics, and the Budyko approach to specify origin of change. The results show that hydrological change is much more important upstream than downstream. The last three decades display a 40% reduction in runoff. This is associated with the direct influence of humans, who are responsible for about 78% of the variation in flow. It appears that climate change contributes to less than about 22%. The combination of increased cultivated land and decreased annual rainfall is the main reason for reduced catchment runoff. Consequently, these effects threaten the sustainable runoff, water in reservoirs, and future water supply in general. Ultimately, the available runoff remains an important parameter and a key indicator to guide the choices of decision-makers and practitioners in current and future climatic conditions. This contributes to supporting sustainable management of remaining water resources.

**Keywords:** climate change; anthropogenic impact; runoff trend

**Citation:** Khemiri, K.; Jebari, S.; Berndtsson, R.; Maalel, K. Is Climate or Direct Human Influence Responsible for Discharge Decrease in the Tunisian Merguellil Basin? *Water* **2021**, *13*, 2748. <https://doi.org/10.3390/w13192748>

Academic Editor: Luís Filipe Sanches Fernandes

Received: 28 August 2021

Accepted: 28 September 2021

Published: 3 October 2021

**Publisher's Note:** MDPI stays neutral with regard to jurisdictional claims in published maps and institutional affiliations.



**Copyright:** © 2021 by the authors. Licensee MDPI, Basel, Switzerland. This article is an open access article distributed under the terms and conditions of the Creative Commons Attribution (CC BY) license (<http://creativecommons.org/licenses/by/4.0/>).

## 1. Introduction

The hydrological cycle is the process upon which all organisms on earth depend for their survival. It is the engine of environmental and ecological conditions on earth [1]. Over the past few decades, several studies have revealed that river flow is linked to many environmental relationships, especially in arid and semiarid areas [2]. Its variations are mainly due to two aspects, namely global climate change and direct human interventions. This contributes to the resulting consequences, a more pronounced scarcity of water resources and more serious environmental deterioration [3–6].

The accelerated global change leaves little time to adjust. Although the need for adaptation to climate change is recognized, there is also a need for adaptation to change affecting land use [7]. Thus, it is essential to understand the causal chains of the processes of river flow variation. As a result, the scientific community has started to analyze the factors behind changes and the possible consequences of these changes [8]. Several factors influence the catchment runoff, including precipitation, temperature, potential evapotranspiration, topography, soil texture, and land use [9]. Human activities are recognized as a major factor affecting river runoff [10]. This appears in deforestation, land use change, soil and water conservation practices, and exploitation of surface and

groundwater reservoirs and water supply [11,12]. Human activities have many negative effects on the environment [13]. This leads, directly or indirectly, to a modification of the quantitative and qualitative characteristics of the river flow. Indeed, changes affecting the land often lead to a significant downward trend in river flow [14]. In addition, the effect of climate change, which modifies precipitation and promotes evapotranspiration by increasing temperature, increases the risk of disturbing the flow of wadis [15]. Thus, the hydrological response to climate change and human activities differs from one area to another [16].

Impact studies of climate change by hydrological models show varying results. Their applications remain limited in watersheds with inadequate data [1]. Thus, conceptual models are replaced by methods based on statistical approaches [17]. The statistical methods are mainly based on trend analysis and the equations of Budyko [18]. During recent years, some research has focused on trend by addressing the influence of length of empirical time series [19,20]. The Budyko approach is based on the concept of climate elasticity [18]. This approach can be used to quantify the sensitivity of river flow to climatic variation. These results will subsequently be useful in designing appropriate management strategies [6]. Additionally, understanding of how flow is affected by land use and climate change is essential to inform adaptive soil and water management.

The Tunisian semiarid context provides an illustrative example of hydrological processes deeply modified by anthropogenic influence [21]. The Merguellil Wadi, the main river in the Merguellil watershed located in central Tunisia, has undergone extremely marked “socio-hydrological” evolution. Its current state is the legacy of a long history of interactions between man and environment [22]. In addition, the watershed is highly vulnerable to climate change that may change river flow [23]. Further, overexploitation of groundwater, agricultural irrigation, and overgrazing can further disrupt the hydrological balance.

In view of the above, the objectives of the present study were partly to improve the understanding on the effects of climate change and direct anthropogenic changes, and partly to assess the impact of length of observed time series by the ITA method (Innovative Trend Analysis) proposed by Şen [24,25]. The ITA method is used in this study since its comparison with conventional methods shows certain advantages [26]. It has been used in the detection of trends for several hydrometeorological variables such as evaporation, river, flow, and precipitation in different regions [26–29]. This method can indicate potential future impacts of climate change, management, and design of hydraulic structures [24].

Assessment of the impact of climate change and direct human activities on streamflow is performed using the approach of Budyko [18] and an NDVI index calculated by multispectral Landsat satellite imagery. The analyses use data from a 40-year period from the Merguellil watershed. The length of time series allows us to compare the hydrological context between shorter study periods in the Tunisian semiarid area. This is one of the first studies that performs a quantitative assessment of the impact of climate change and direct human activity on streamflow variation in the Merguellil Wadi.

## 2. Materials and Methods

### 2.1. Study Area

The watershed of the Merguellil Wadi is located in central Tunisia. It covers an area of 1183 km<sup>2</sup>. The El Haouareb dam, built in 1989, has a natural outlet (Figure 1) and retains all water from Merguellil Wadi [30]. The shape of the watershed is almost triangular, the base being downstream (Figure 1). The main stream of the Merguellil Wadi directly drains most of the basin, the tributaries of some importance being located on the right bank. The river bed of the Wadi is very sensitive to erosion [31]. The altitude varies between 200 and 1200 m with an average of 500 m (Figure 1).

The watershed is semiarid, characterized by very high spatial and temporal variability of precipitation. Figure 2 shows the annual precipitation of the nearby Kairouan station during the period 1950–2020, including the study period 1976–2017. The displayed long-term rainfall averages aim to assess the representativity of the study period in relation to long-term rainfall conditions. The average annual precipitation during the 70 years is 307 mm (standard deviation  $\pm 108$  mm). The average for the period 1976–2017 is equal to 290 mm (standard deviation  $\pm 89$  mm). Thus, it can be said that the study period is representative for longer periods. In Tunisia, the rainfall regime is often subject to a semi-periodicity of about 10 years [32]. In addition, since the 1950s, Tunisia has experienced a decrease of 5% per decade in annual rainfall [33]. The ten-year average precipitation (Figure 2) shows that there are successive periods of sequential surplus, deficit, and periods close to the long-term average. Figures 3 and 4 show the annual and intra-annual variability of precipitation (P), temperature (T), potential evapotranspiration ( $E_0$ ), and river flow (Q) in the Merguellil Wadi.

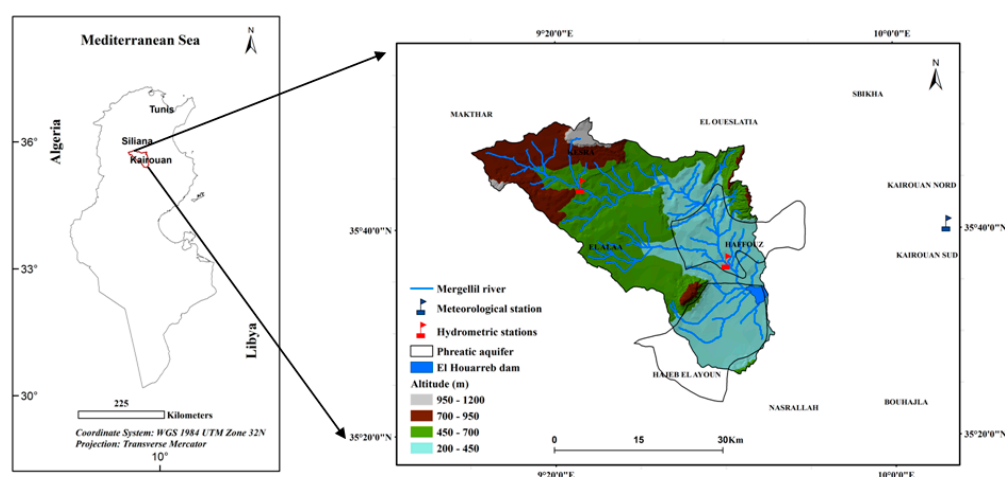


Figure 1. Location and topography of the Merguellil Wadi in central Tunisia.

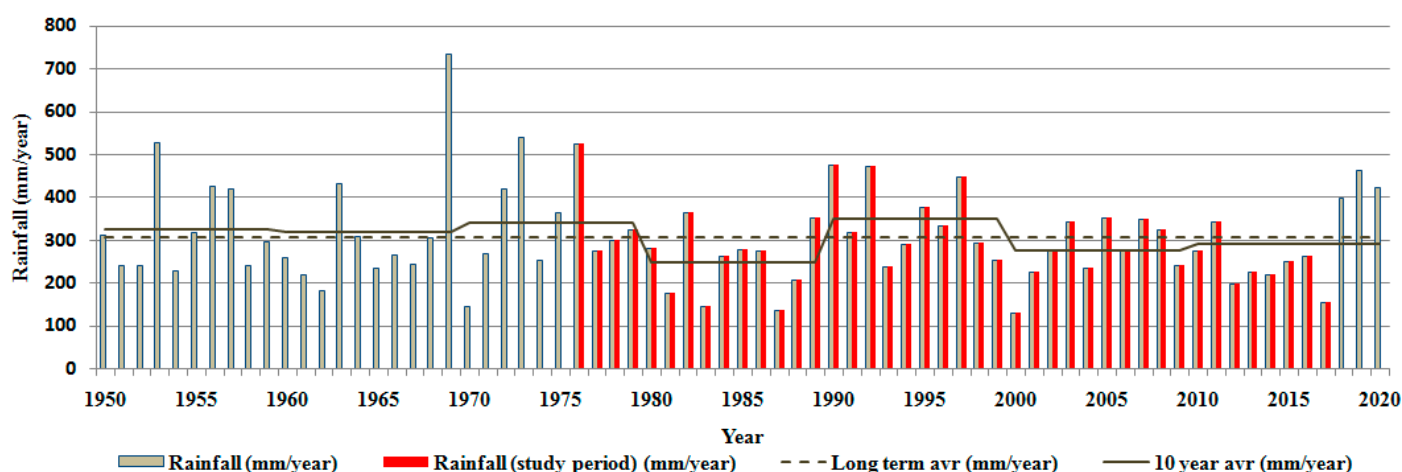


Figure 2. Average annual rainfall at Kairouan during 1950–2020 (Source: Tunisian Meteorological Institute).

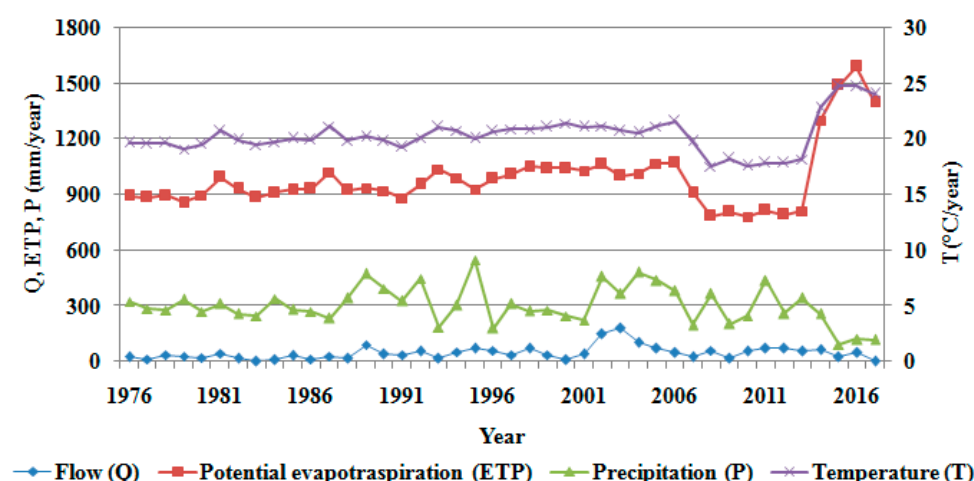


Figure 3. Annual variability of different hydroclimatic variables in the Merguellil Wadi.

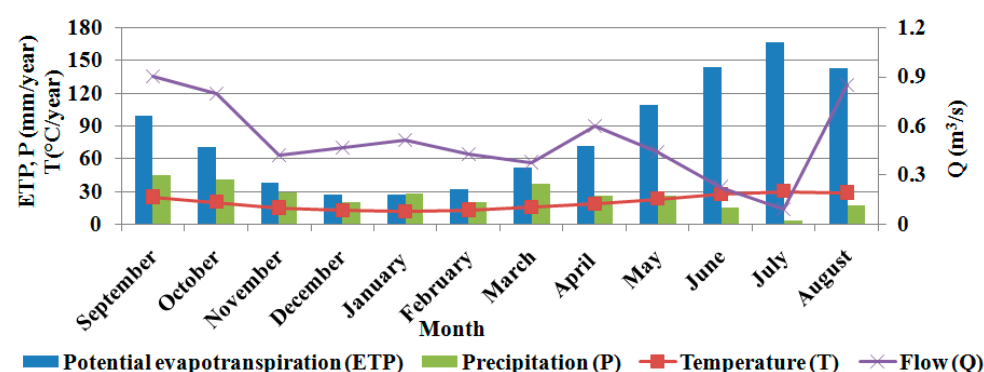


Figure 4. Annual variation of ETP, P, T, and Q in the Merguellil Wadi.

Rainfall is often intense, especially in spring and autumn, which cause flooding [34]. The estimated peak flow during an exceptional flood event in September 1969 reached 3000 m<sup>3</sup>/s at Haffouz [35]. Periodic river flow of the Merguellil Wadi supplies the El Haouareb Dam that itself feeds the downstream aquifer of the Kairouan plain. The aquifer is heavily exploited for irrigated agriculture and drinking water supply. There are two phreatic aquifer systems in the watershed, the Bouhefna–Haffouz–Chérichira (BHC) and the Ain Beidha (Figure 1). Little is known about their recharge and exchange, and links between river flow and the aquifer [36]. The soil texture can be classified into four main parts, namely alternating limestone–marl formations giving silty–clay soils with active clays conditioning active processes of soil degradation [37,38]. The geology is complex and mainly composed of limestone, marl–limestone, and marly sedimentary formations of the Cretaceous and Eocene [39,40]. The soil and water conservation practices consist of grass strips, stone barriers, contour ridges, and 44 lakes and hill dams. These structures occupy 260.45 km<sup>2</sup> or 22% of the watershed area [41].

## 2.2. Data Used

Rainfall and runoff data were used from the Skhira and Haffouz stations (Figure 1). They were collected by the General Directorate for Water Resources [42]. Temperature (T) data were taken from the Tunisian Meteorological Institute [43] database for the Kairouan station (Figure 1 and Table 1). Data gaps were less than 3% and filling of missing data was performed by multiple regression [44]. The daily data covered a 42-year period (1976–2017). The hydrological year begins on 1st September and ends on 31st August.

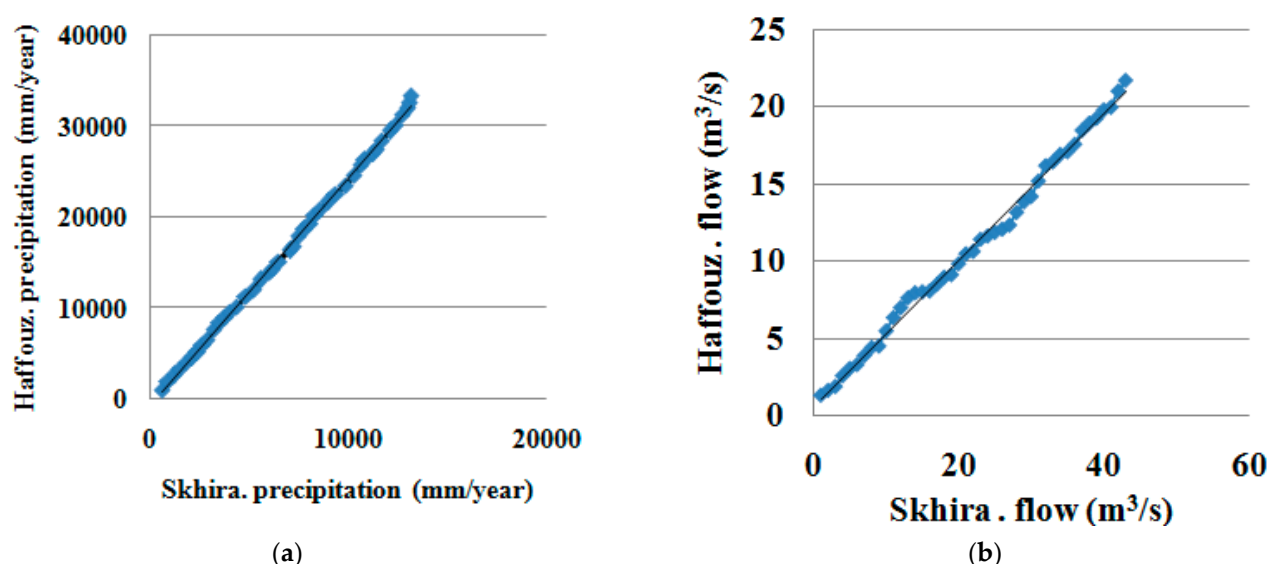
**Table 1.** Characteristics of stations used.

Station	Type	Longitude	Latitude	Altitude (m)
Kairouan SM	Meteorological	10°10'42"	35°67'59"	66
Haffouz Telepherique	Hydrometric	07°19'19"	35°37'58"	250
Skhira	Hydrometric	07°02'49"	35°44'24"	600

Table 2 shows descriptive statistics of the river flow, rainfall, evapotranspiration, and temperature series. The rainfall upstream in the basin (Skhira station) is significantly larger compared to the downstream (Haffouz station) due to orographic effects [45]. Figure 5 shows double mass curves for annual precipitation and river flow at the Skhira and Haffouz stations and approximate homogeneity of the data [46–48].

**Table 2.** Descriptive statistics of data used for the study period (1976–2017).

Statistic	River Flow (m <sup>3</sup> /s)		Precipitation (mm/year)		Temperature (°C/year)	Potential Evapotranspiration (mm/year)
	Skhira	Haffouz	Skhira	Haffouz	Kairouan	Kairouan
Mean	0.28	0.53	395.1	289.54	20.27	982.6
Variance	0.04	0.11	24,402	7904	2.71	30,086
Standard deviation	0.21	0.34	156.2	88.91	1.65	173.5
Coefficient of variation	0.75	0.64	0.40	0.31	0.08	0.18
Std. error of mean	0.03	0.05	23.8	13.5	0.25	26.5
Skewness(Pearson)	0.60	0.41	0.69	0.39	0.42	0.86
Minimum	0.01	0.05	116.0	128.7	17.53	780.3
Maximum	1.06	1.40	844.2	524.2	24.80	1591.6
Autocorrelation Coefficient r(1)	0.51	0.16	0.25	0.18	0.78	0.81

**Figure 5.** Double mass curves for, (a) precipitation, and (b) river flow.

To analyze land use dynamics, we used multispectral Landsat 1, 5, and 8 satellite data. These images were used for calculation of NDVI index [49,50]. Landsat 1 MSS (Multi-Spectral Sensor) image was acquired for 21 July 1976, Landsat 5 TM (Thematic Mapper), and Landsat 8 OLI-TIRS (Operational Land Imager—Thermal Infrared Sensor) were for 19 July 1996 and 21 July 2016, respectively. The images have a spatial resolution of 30 m. All images were from July. This date coincides with start of the dry season and end of the rainy season. This made it possible to avoid effects of annual vegetation and to

improve the knowledge on behavior and distribution of vegetation cover. Landsat images are downloaded free of charge from the USGS website (<https://earthexplorer.usgs.gov> (accessed on October 3 2019)).

### 2.3. Runoff Trend Analysis

Identification of the flow trend was performed by using the ITA method (Innovative Trend Analysis) proposed by Şen [24,25]. It offers advantages over traditional statistical tools and its graphics present more detail by characterizing extreme events. In the ITA method, recorded flow data are divided into two equal parts from start to end of the time series. The two subseries are sorted separately in ascending order. For estimating the trend rate, the slope  $S_{ITA}$  and trend indicator  $T_{ITA}$  are calculated by:

$$S_{ITA} = \frac{2(\bar{X}_1 - \bar{X}_2)}{n} \quad (1)$$

$$T_{ITA} = \frac{1}{n} \sum_{i=1}^n \frac{10(X_i - \bar{X}_1)}{\mu} \quad (2)$$

where  $n$  is sample size,  $X_i$ ,  $\bar{X}_1$ , and  $\bar{X}_2$  are values and averages of the first and second half of the time series, respectively,  $\mu$  is average of the first half of the time series.

The ITA method detects trends over a time series across two divided subseries of equal lengths. In addition, the standard deviation of the trend slope deviation formula assumes that variation is constant. This assumption is not valid for asymmetric and dependent series [51,52]. Therefore, ITA detects trends on a main time series with equal sub-series length [53]. Thus, we divided the 42-year study period into three periods: 20 years (1976–1995; 1996–2017), 30 years (1976–2005), and 40 years (1976–2017), and we verified that the series are not autocorrelated.

To implement the ITA method, the open source “trendchange” library was developed in R language and made available via the CRAN repository.

### 2.4. Climate Elasticity of Annual Flow

The climate elasticity of annual flow  $\varepsilon$  is an indicator of sensitivity of long-term hydrological systems to climatic fluctuation. The use of  $\varepsilon$  is informative for estimation of the impact of climate change on the hydrological system. It is a non-parametric estimator that calculates the elasticity value directly from time series data of annual flow in relation to the variability of precipitation or potential evapotranspiration [54,55]. Its evaluation offers an opportunity for efficient management of water resources [56,57]. It is calculated by:

$$\varepsilon = \frac{dQ/Q}{dX/X} = \frac{dQ}{dX} \frac{X}{Q} \quad (3)$$

where  $\bar{X}$  and  $\bar{Q}$  are precipitation or potential evapotranspiration and average annual flow for the entire study period, respectively;  $X_i$  and  $Q_i$  are annual precipitation or potential evapotranspiration and flow for the  $i$ th year, respectively.

The climate elasticity of annual flow, Equation (3), can be expressed according to the studies of Sankarasubramanian et al. [55] and Zheng et al. [54] in a non-parametric form:

$$\frac{\Delta Q_i}{\bar{Q}} = \varepsilon \frac{\Delta X_i}{\bar{X}} \quad (4)$$

Thus, Equation (4) can be rewritten as:

$$\varepsilon = \frac{\bar{X} \sum (X_i - \bar{X})(Q_i - \bar{Q})}{\bar{Q} \sum (X_i - \bar{X})^2} = \rho_{XQ} \left( \frac{c_Q}{c_X} \right) \quad (5)$$

where  $\rho_{X,Q}$  is the correlation coefficient between  $C_X$  and  $C_Q$ . These are the coefficients of variation for X and Q, respectively. Thus, these three parameters are calculated as:

$$\rho_{X,Q} = \frac{\sum (X_i - \bar{X})(Q_i - \bar{Q})}{\sqrt{\sum (X_i - \bar{X})^2 \sum (Q_i - \bar{Q})^2}} \quad (6)$$

$$C_Q = \frac{\sqrt{\sum (Q_i - \bar{Q})^2 / n}}{\bar{Q}} \quad (7)$$

$$C_X = \frac{\sqrt{\sum (X_i - \bar{X})^2 / n}}{\bar{X}} \quad (8)$$

Potential evapotranspiration was calculated by the Thornthwaite method [58,59]:

$$E_0 = \left[ 16 \left( \frac{10 \bar{T}}{I} \right)^a \right] F(m, \varphi) \quad (9)$$

where  $E_0$  (mm/month) is the average evapotranspiration of the month m (m = 1 to 12);  $\bar{T}$  is interannual average temperature of the month in °C; I is annual thermal index, and  $F(m, \varphi)$  is a corrective factor depending on month (m) and latitude ( $\varphi$ ).

The parameters a, I and i are calculated as:

$$a = 0.016 \times I + 0.5 \quad (10)$$

$$I = \sum_{m=1}^{12} i(m) \quad (11)$$

$$i(m) = \left[ \frac{\bar{T}(m)}{5} \right]^{1.514} \quad (12)$$

$$F(m, \varphi) = \left( \frac{L}{12} \right) \left( \frac{N}{30} \right) \quad (13)$$

where N is the number of days in the month and L is the average day length (hours) of the month.

## 2.5. Connection between Climate Change, Anthropogenic Activity, and Streamflow

At watershed scale, streamflow can be simulated as a function of climate change (C) and anthropogenic activity (H) as [60]:

$$Q = f(C, H) \quad (14)$$

where Q is flow; C represents integrated effect of climatic variables; H represents integrated effects of human activities. Therefore, the flow variation can be approximated by [17]:

$$\Delta Q = \Delta Q_C + \Delta Q_H \quad (15)$$

where  $\Delta Q$  is total variation of streamflow;  $\Delta Q_C$  is change in streamflow due to climate change, and  $\Delta Q_H$  is change in flow caused by anthropogenic activities. The total variation of river flow is determined by:

$$\Delta Q = \Delta Q_{\text{obs},2} - \Delta Q_{\text{obs},1} \quad (16)$$

where  $\Delta Q_{\text{obs},1}$  and  $\Delta Q_{\text{obs},2}$  are the annual discharge observed in period P1 and P2, respectively.

Precipitation (P) and potential evapotranspiration ( $E_0$ ) are the dominant controlling factors for average annual water balances [6,15,18]. The variation in annual flow due to variation in annual average precipitation and potential evapotranspiration is determined by:



$$\Delta Q_e = (\varepsilon_p \Delta P / P_{obs,1} + \varepsilon_{E_0} \Delta E_0 / E_{0,obs,1}) Q_{obs,1} \quad (17)$$

where  $\varepsilon_p$  and  $\varepsilon_{E_0}$  are the elasticity of precipitation and potential evapotranspiration of runoff. The  $\Delta P$  and  $\Delta E_0$  are the variation in precipitation and potential evapotranspiration. The  $\Delta P$  and  $\Delta E_0$  are determined by:

$$\Delta P = P_{obs,2} - P_{obs,1} \quad (18)$$

$$\Delta E_0 = E_{0,obs,2} - E_{0,obs,1} \quad (19)$$

where  $P_{obs,1}$ ,  $P_{obs,2}$ ,  $E_{0,obs,1}$  and  $E_{0,obs,2}$  are precipitation and potential evapotranspiration for the period P1 and P2, respectively.

## 2.6. Identification of Land Use Dynamics by NDVI Index

The normalized vegetation index (NDVI) was used to assess the importance of biomass and chlorophyll activity. The NDVI ranges from  $-1$  to  $+1$ . Negative values correspond mainly to open water. Values close to zero are formed mostly of rock, roads, and bare soil. Moderate values (0 to 0.2) represent bare soil up to the early stage of vegetation growth, while values 0.2 to 0.8 correspond to plant variability. Values close to  $+1$  (0.8 to 1) indicate forest areas or dense vegetation [61,62]. The NDVI index was used to assess the dynamics of land use in the Merguellil watershed. It was calculated by:

$$NDVI = (PIR - R) / (PIR + R) \quad (20)$$

where PIR is the infrared and R the red spectral band.

## 3. Results

### 3.1. Analysis of Trend in River Flow

The annual trend in river flow for the four observation periods (P1: 1976–1995; P2: 1996–2017; P3: 1976–2005; P4: 1976–2017) using the ITA method for the two stations Haffouz and Skhira is shown in Tables 3 and 4 and Figure 6. For periods P1, P3, and P4, average annual flow followed an increasing trend for the upstream Skhira station. This trend is significant with a 95% confidence interval during period P3 and P4. It can be seen from Table 3 and 4 that the slopes of the ITA method are dominated by positive values, namely, P1 (0.01 m<sup>3</sup>/s), P3 (0.01 m<sup>3</sup>/s), and P4 (0.02 m<sup>3</sup>/s). A decreasing trend characterized the downstream Haffouz. As for period P2, we observe a significant annual decrease for both stations. Extreme flows (min) show an increasing trend upstream in the watershed for the different periods. The maximum flow followed a decreasing trend for the three periods P2, P3, and P4, with an average slope of 0.2 m<sup>3</sup>/s. At the downstream of the watershed the significant trend was decreasing, especially in the thirty- and forty-year periods.

Like annual flow, the hydrological response of seasonal flow is much greater at the upstream than the downstream. The trend for period P1, P3, and P4 is greater in winter than during the other three seasons. The fall and summer seasons are characterized by a significant increasing trend during the 30- and 40-year periods at the upstream of the watershed. This trend is weaker at the downstream with a reduction of over 60%. Regarding the period P2, the trend is significantly decreasing.

On a monthly scale, in the upstream, September characterizes the fall trend. December and February play a primary role in the winter trend. The summer trend is influenced by July. In the downstream, January and February influence the winter trend. In addition, May and July characterize the trend of spring and summer, respectively.

**Table 3.** Trend analysis using the ITA method for upstream of the Merguellil watershed (Skhira station), m<sup>3</sup>/s.

P1: 1976–1995	P2: 1996–2017	P3: 1976–2005	P4: 1976–2017
---------------	---------------	---------------	---------------



	S	CL	Sig	S	CL	Sig	S	CL	S	CL	Sig	
Annual	0.01	±0.01	+	−0.02	±0.005	−	0.01	±0.001	+	0.02	±0.0036	+
September	0.04	±0.01	+	0.01	±0.027	+	0.045	±0.008	+	0.01	±0.001	+
October	−0.007	±0.005	−	−0.01	±0.011	−	0.016	±0.002	+	0.01	±0.002	+
November	−0.004	±0.001	−	0	±0.002	+	0.09	±0.002	+	0.01	±0.0018	+
December	0.003	±0.007	+	−0.02	±0.003	−	0.012	±0.004	+	0.005	±0.002	+
January	0.02	±0.008	+	−0.08	±0.016	−	0.04	±0.007	+	0.01	±0.002	+
February	0.02	±0.005	+	−0.03	±0.003	−	0.026	±0.003	+	0.004	±0.0008	+
March	0.0006	±0.007	+	0	±0.002	+	−0.01	±0.001	−	0.0007	±0.0008	+
April	−0.01	±0.004	−	−0.01	±0.006	−	−0.0004	±0.002	−	0.0003	±0.001	+
May	0.03	±0.002	+	0.01	±0.003	+	−0.002	±0.0023	−	−0.0007	±0.001	−
June	−0.003	±0.002	+	−0.06	±0.033	−	0.02	±0.019	+	0.01	±0.007	+
July	0.02	±0.002	+	0	±0.0005	−	0	±0.0015	−	0.0005	±0.0034	+
August	0.02	±0.014	+	−0.02	±0.0108	−	0.03	±0.003	+	0.01	±0.0038	+
Autumn	0.009	±0.002	+	0	±0.0071	+	0.023	±0.02	+	0.01	±0.002	+
Winter	0.015	±0.004	+	−0.04	±0.004	−	0.026	±0.002	+	0.008	±0.001	+
Spring	0.005	±0.004	+	0	±0.0008	+	−0.004	±0.004	−	−0.0001	±0.00067	−
Summer	0.014	±0.003	+	−0.03	±0.008	−	0.015	±0.001	+	0.003	±0.002	+
Minimum discharge	0.12	±0.04	+	0.37	±0.35	+	0.42	±1.1	+	1.34	±1.18	+
Maximum discharge	0.99	±0.14	+	−0.25	±0.15	−	−0.26	±0.1	−	−0.09	±0.03	−

S: trend slope; CL: lower and upper confidence interval for  $\alpha = 5\%$ ; Sig: trend sign.

**Table 4.** Trend analysis using the ITA method for downstream of the Merguellil watershed (Haffouz station), m<sup>3</sup>/s.

	P1: 1976–1995			P2: 1996–2017			P3: 1976–2005			P4: 1976–2017		
	S	CL	Sig	S	CL	Sig	S	CL	Sig	S	CL	Sig
Annual	−0.008	±0.004	−	0.01	±0.001	+	−0.006	±0.0015	+	−0.06	±0.0008	+
September	0.05	±0.006	+	−0.03	±0.041	−	0.05	±0.005	+	0.0009	±0.006	+
October	−0.02	±0.001	−	−0.02	±0.0129	−	−0.03	±0.008	−	0.001	±0.005	+
November	−0.05	±0.0096	−	0.03	±0.015	+	−0.09	±0.0056	−	0.009	±0.005	+
December	0.004	±0.004	+	0.04	±0.0319	+	0.018	±0.003	+	0.02	±0.01	+
January	−0.007	±0.002	−	−0.14	±0.04	−	0.07	±0.01	+	0.03	±0.006	+
February	0.027	±0.015	+	−0.07	±0.006	−	0.05	±0.01	+	0.005	±0.007	+
March	−0.07	±0.005	−	0.01	±0.008	+	−0.02	±0.006	−	−0.007	±0.003	−
April	−0.11	±0.011	−	−0.02	±0.009	−	−0.04	±0.005	−	−0.01	±0.003	−
May	0.05	±0.007	+	−0.04	±0.004	−	−0.009	±0.015	−	−0.004	±0.007	−
June	0.003	±0.003	+	−0.03	±0.0023	−	−0.003	±0.002	−	0.006	±0.0015	+
July	0.011	±0.003	+	0.01	±0.0019	+	7.38	±6.2	+	0.001	±0.001	+
August	0.016	±0.009	+	0.07	±0.027	+	0.003	±0.004	+	0.02	±0.003	+
Autumn	−0.006	±0.005	−	−0.04	±0.0036	−	0.02	±0.006	+	0.003	±0.003	+
Winter	0.007	±0.004	+	−0.05	±0.029	−	0.04	±0.002	+	0.02	±0.003	+
Spring	−0.04	±0.02	−	−0.01	±0.006	−	−0.02	±0.004	−	−0.01	±0.003	−
Summer	0.01	±0.007	+	0.01	±0.005	+	0.002	±1.38	+	0.005	±0.001	+
Minimum discharge	−0.12	±0.04	−	0.24	±0.13	+	−1.35	±2.27	−	−0.01	±0.02	−
Maximum discharge	−1.72	±0.54	−	−0.56	±0.39	−	−0.18	±0.26	−	−0.03	±0.12	−

S: trend slope; CL: lower and upper confidence interval for  $\alpha = 5\%$ ; Sig: trend sign.

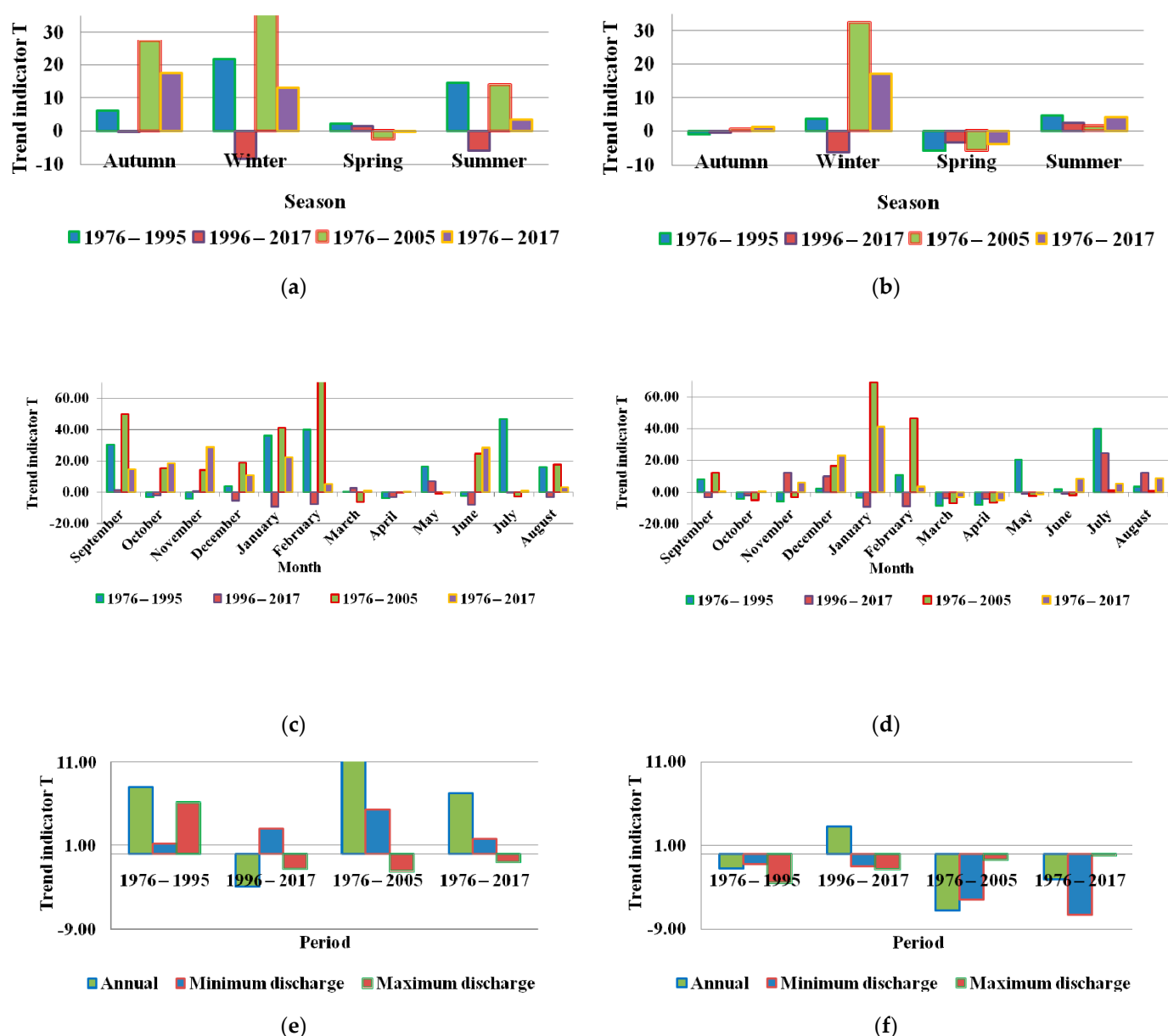


**Figure 6.** Trend analysis using the ITA method for different time steps (season, monthly, annual, and max and min) according to the four study periods for Skhira (a,c,e) and Haffouz (b,d,f).

### 3.2. Climate Elasticity of Annual Flow

To assess the impacts of climate change on the river flow of the Merguellil Wadi, the climate elasticity of the flow in relation to annual precipitation and potential evapotranspiration was calculated for the two periods using Equation (5) for the two stations Haffouz and Skhira. The  $\varepsilon$  is summarized in Table 5. The results of the climate elasticity for the streamflow vary from upstream to downstream of the watershed (Table 5). This translates into that a 10% change in precipitation implies a change from −6.2 to 16% in average annual flow for the Haffouz station and from 9 to 12% for the Skhira station during the two periods P1 and P2. A 10% decrease in potential evapotranspiration is associated with a −6 to 16.5% increase in streamflow (Table 5).

**Table 5.** Annual average hydrological variables and climate elasticity for the different periods of the Merguellil watershed.

Hydrological Station	Period	Mean of Hydrological Variable	Climate Elasticity
----------------------	--------	-------------------------------	--------------------

		Q (m <sup>3</sup> /s)	P (mm)	E <sub>0</sub> (mm)	ε <sub>p</sub>	εE <sub>0</sub>
Skhira	1976–2017	0.24	321.3	985.5	1.26	−0.26
	1976–1995	0.32	321.9	928.3	0.93	0.07
	1996–2017	0.17	284.6	1037.3	1.25	−0.25
Haffouz	1976–2017	0.50	302.5	985.5	1.35	−0.35
	1976–1995	0.45	321.5	928.3	−0.65	1.65
	1996–2017	0.56	336.0	1037.3	1.62	−0.62

### 3.3. Impact of Climate Change and Anthropogenic Activities on Streamflow

Table 6 illustrates the impact of climate change and anthropogenic activities on river flow in the Merguellil watershed. Indeed, by using Equation (17), in the upstream of the watershed, a decrease of 38 mm in precipitation results in a decrease of 0.17 mm in streamflow (Skhira). Thus, an increase of 109 mm in potential evapotranspiration will decrease streamflow depth by 0.03 mm (Table 6). Similarly, for the downstream of the Merguellil watershed, increase in precipitation and evapotranspiration results in a small increase in streamflow (Table 6).

**Table 6.** Annual average hydrological variables and climate elasticity for the different periods of the Merguellil watershed.

Hydrometric Station	$\Delta Q$ (mm)	$\Delta P$ (mm)	$\Delta E_0$ (mm)	$\Delta Q_p$ (mm)	$\Delta Q_E$ (mm)	$\Delta Q_e$ (mm)	$\Delta Q_e/\Delta Q$	$\Delta Q_H$ (mm)	$\Delta Q_H/\Delta Q$
Skhira	−23.9	−37.9	108.9	−0.17	−0.03	−5.2	21.6%	−18.7	78.3%
Haffouz	15.5	15.65	108.9	0.07	−0.04	0.6	3.9%	14.8	96.1%

The cumulative effect of changes in precipitation and potential evapotranspiration results in a −5.2 to 0.6 mm increase in streamflow, i.e., a variation of 21.6 to 3.9% compared to observed variation (Table 6) at Skhira and Haffouz stations, respectively. Thus, it is estimated that anthropogenic activities account for more than 78% of the variation in streamflow for the Merguellil watershed (Table 6).

### 3.4. Impact of the Dynamics of Land Use on Streamflow

A decreasing trend in inflow to the El Houarreb Dam has been observed since the early 1970s. This decrease implies that the flow could be affected by anthropogenic activities more than climate change. In the present study, we assume that primary anthropogenic activity affects the flow of Merguellil Wadi through water withdrawal, land use, and land use change. The results of the calculation of the NDVI index for the Merguellil watershed for 1976, 1996, and 2016 are grouped together in Figure 7 and Table 7.

**Table 7.** Total area of NDVI index classes for 1976, 1996, and 2016.

NDVI	Area					
	1976		1996		2016	
	(ha)	(%)	(ha)	(%)	(ha)	(%)
<0	3.9	0	316.6	0.2	11.8	0
0–0.2	85,905.9	72.6	69,819.7	59.1	102,294.8	86.5
0.2–0.8	32,411.0	27.4	48,184.7	40.7	16,014.3	13.5

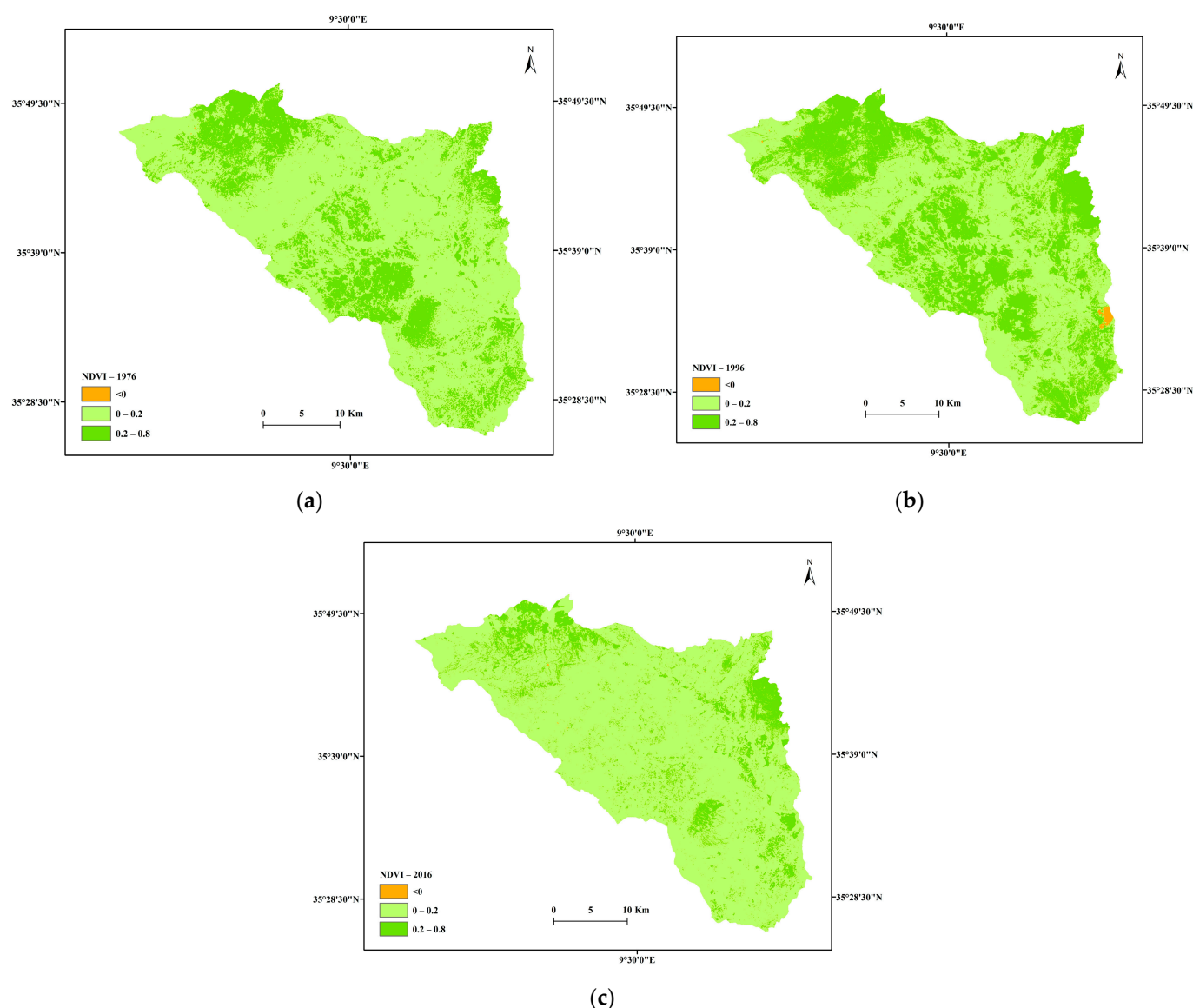


**Figure 7.** NDVI maps for the Merguellil watershed during (a) 1976, (b) 1996, and (c) 2016.

During the study period, the Merguellil watershed underwent a change in land use. Indeed, the NDVI index is between  $-1$  and  $0.8$ , with an absence of values close to  $1$ . The NDVI class between  $0$  and  $0.2$  has experienced a significant increase, while water bodies ( $\text{NDVI} < 0$ ) have been reduced (Table 7). During the period 1976–1996, vegetation cover ( $0.2 < \text{NDVI} < 0.8$ ) and open water bodies ( $\text{NDVI} < 0$ ) increased by  $13$  and  $0.3\%$ , respectively. However, uncovered or bare surfaces ( $0 < \text{NDVI} < 0.2$ ) decreased by  $13\%$  (Table 7). This is a result of conversion of denuded areas into forests, crops, and arboriculture as well as the construction of the El Houarreb Dam in 1989. However, during the period 1996–2016, the NDVI class between  $0.2$  and  $0.8$  experienced a decrease of  $27\%$ . At the same time, land covered with vegetation increased by  $27\%$ .

#### 4. Discussion

Analysis of flow trend by the ITA method in the Merguellil watershed over the periods of 20, 30, and 40 years shows that the impact of time series length on the magnitude of trends is substantial. In fact, on a monthly scale a positive trend for P1 and negative for P2 for the 20-year period is not found in the 30 and 40-year periods, respectively. Indeed, at longer observation periods ( $\geq 30$  year), the trend is increasing for annual flow. How-

ever, it is decreasing for extreme values of flow rates. In addition, one can notice a concordance of the magnitude of the trends during the four periods. This concordance appears, increasing in the watershed, particularly in spring during March and April. Downstream in the watershed, the concordance of magnitudes of trends characterized autumn, summer, and September, October, March, April, and June. The ITA method has certain advantages for flow series analyses. The approach allows for more detailed interpretation of trend detection, which is useful for identifying hidden trends over time. The ITA method identified statistically significant upward and downward trends over the 30-year period. In this framework, we observed a high degree of connection of magnitudes of the trends for the 20 and 40-year series.

The 20-year trend magnitude results show a negative sign that is statistically significant. This is mainly due to the deficit years experienced in the study area (Figure 2). Consequently, these results reflect the hydrological variability of the Merguellil watershed and not the hydrological trend linked to climate change. The 30-year series analysis identified a clear trend. Similarly, the 40-year series showed rather moderate amplitudes (Figure 6). In conclusion, the 30 and 40-year series showed pronounced and moderate impact of climate change, respectively.

Statistical results of the study show that the hydrological response of stream flow is much greater upstream than downstream. The last three decades illustrate a 40% reduction in inflow to the dam. This is in accordance with what has been published in the yearly hydrological reports by the Kairouan hydrological department. Indeed, the Merguellil Wadi recorded zero flow for the first time in 1979 at Haffouz. Thus, a clear downward trend is observed between 1976–1977 and 1988–1989. This follows a succession of years of deficit due to the reduction in rainfall events of more than 30 mm [62]. In addition, despite the surplus period over five consecutive years from 2002–2003 to 2006–2007, an absence of decrease in rainfall over the watershed and across Tunisia was recorded [13,63–66]. Thus, the Merguellil Wadi remains in a vulnerable situation.

Climate elasticity of annual flow expresses the percentage change in flow as a function of percentage change in climatic variables. It is proportional to precipitation, temperature, and increases with temperature if precipitation decreases and decreases with temperature if precipitation increases [67]. The results of the present study show that the climate elasticity of flow is variable. This lack of stationarity contradicts the conclusion of Sankarasubramanian et al. [55]. In addition, it can take negative signs (Table 5). This means that the reduction in input is combined with an increase in temperature, which tends to increase evapotranspiration, followed by a decrease in precipitation [68,69]. Therefore, the availability of water in the study area will likely be more critical in the future with current projections of global warming. An increase of 2 °C is likely to be followed by a significant decrease in water availability by 2 to 15% [70].

Our results suggest that the effect of climatic factors on the average annual flow increases from upstream to downstream of the watershed. This agrees with the results of Tsai [71]. Indeed, it is quite natural that our estimates of the effects of precipitation and evapotranspiration on the average flow in the Haffouz station differ from those estimated in the north of the watershed, at the Skhira station. A forest cover and an altitude, which varies from 700 to 1200 m, characterize the north. In addition, the effect of temperature on low water flow in the Haffouz region, an area characterized by a permeable soil texture, is greater than that on the average flow in the Skhira station.

The elasticity of potential evapotranspiration throughout the study period for the upstream is higher than downstream of the watershed. This indicates that the response of the Merguellil Wadi is more sensitive to potential evapotranspiration than precipitation. Certainly, evapotranspiration through vegetation significantly affects the flow, especially at the end of the growing season [72]. In general, the effects of non-climatic factors include changes in land use and human activities have been shown to be influencing factors for water supply. Vegetation changes in the Merguellil watershed (Figure 7) come about because of government intervention in the Kairouan region. This intervention aims

to improve the country's self-sufficiency in certain products (vegetables, fruits, and cereals) and the supply of agricultural products to feed the livestock [73]. Thus, an extension of the cultivated area following governmental investments in water saving equipment linked to the development of drip irrigation between 1999 and 2005 [74].

Although, the results of the combination of the effects of climate change and land use show a reduction in water supplies to the basin. Human contribution plays an important role for the Merguellil watershed [22]. The growing demand of water for agricultural, domestic, and industrial purposes has led to overuse of surface and groundwater. The withdrawal of surface water will reduce the flow directly. Thus, the overexploitation of groundwater leaves a void to be filled by surface runoff, thus reducing the flow of watercourses.

Soil texture plays a role in the evolution of runoff. Indeed, upstream of the watershed (Skhira station), the riverbed of the Merguellil Wadi is formed by hard rocks with a stable section. Downstream, at the Haffouz station, the Merguellil bed is wide, formed by unstable sandy formations. It is then exposed to erosion phenomena, which means that the section changes shape almost at each passage of a flood [34]. Water for domestic, irrigation, industrial, and tourist use is being taken from deep groundwater of the Merguellil watershed. In addition, the disturbance of the hydrological balance in the study area can be explained by feedback from local residents following the disappearance of the low flow of Wadi Merguellil and its drying up since 1981 [34,75]. This consequence appeared following a political strategy to draw down the groundwater system of Bouhefna, located in the center of the study area (Figure 1), since the mid-1970s. This strategy aims to reduce water losses by evapotranspiration and for hydrogeological purposes. It therefore induces excessive hydrodynamic exploitation of underground resources [34]. This is planned in the expansion of agricultural pumping along the Wadi, by abandoning traditional irrigation canals, installing motor pumps, and setting up deep boreholes in the alluvium of the Wadi or wells on the banks from the 1980s. The transfer of water from Bouhefna to the coastal regions presents another explanatory factor for the hydrological changes experienced in the Merguellil watershed that is widely contested by the local population [21].

In a semiarid region such as the Merguellil watershed, the hydrological processes are characterized by an extreme spatiotemporal variability (e.g., [76]). The high rainfall variability requires human intervention to mitigate the landscape change. We particularly mention soil and water conservation practices and careful land use/land cover management. Indeed, surface runoff is generated by exceptional events that are rare but complex [77,78]. However, only extreme events produce significant runoff.

The expansion of water and soil conservation management has led to a marked decrease in runoff in the Merguellil watershed [41]. Many investigations have focused on the variability of runoff coefficient (e.g., [79–81]). In this regard, by analyzing 114 comparable events over the period 1989–2010, Ogilvie et al. [82] estimated a 40% reduction in the runoff coefficient following the expansion of water and soil conservation practices since 1996 with a decrease of 25% in annual flow at the basin outlet. Lacombe et al. [83] estimated that the sharp drop in flow arriving at the El Haouareb Dam over the past 40 years is due to a reduction of runoff generated by events below 40 mm from 28 to 32% and a reduction of 41–50% for all events over the period 1989–2005.

In conclusion, this research shows the importance of the flow to identify the impact of climatic change and anthropogenic activities in a Tunisian semiarid context. Thus, it is recommended that the length of the hydrological series should not be less than 30 years when analyzing the impact of climate change on streamflow. This can therefore serve as a benchmark for future research. In addition, this study confirms the importance of using seasonal and monthly flow data in trend analysis, rather than simple annual averages which may sometimes not reveal the full spatiotemporal complexity of flow trends.

Ultimately, this study identifies the importance of the continuity of research, which has been initiated in the Merguellil watershed for more than 50 years. This continuity has

made it possible to show that anthropogenic effects make water scarcity a permanent situation in a semiarid context. The purpose of this is to guide rural development agents to consider water management and saving models adapted to climate change and land use to avoid finding themselves in similar situations in the future.

## 5. Conclusions

This study assessed impacts of climate change and direct human activities on streamflow in the Merguellil watershed. Trend at monthly, seasonal, and annual time scales was studied using the ITA method over the period 1976–2017 divided into periods of about twenty years each (P1: 1976–1995; P2: 1996–2017), about thirty years (P3: 1976–2005), and about forty years (P4: 1976–2017). The purpose was, on the one hand, to provide a length of series capable of informing us about the impact of climate change and on the other hand, allowing us to compare the hydrological contexts between the different study periods. Analysis of the trend shows that the hydrological response of flows is much greater upstream than downstream. The average annual flow towards the outlet of the watershed, the El Houarreb Dam, has decreased significantly over the past thirty years by about 40%. Extreme low flows have increased in high and medium altitudes, thus constituting a constant pressure on the availability of water resources in the watershed where the residents depend on agricultural activities. Strong points of this study are the precision of the detection of long-term trends. A 20-year time series reflects the hydrological variability and the characteristics of the watershed. This observation time, however, does not reflect the hydrological trends linked to climate change. Indeed, only series of 30 years and more can clearly and explicitly identify the impact of climate change. From the 40-year data, we can identify climatic impact that is more objective for an optimal management of water resources. In addition, this study confirms the importance of using seasonal and monthly flow data in trend analysis. Indeed, simple annual averages cannot reveal the spatiotemporal complexity of flow trends. The calculation of the NDVI index by using the three Landsat images provided an overview for a global qualitative analysis of the contribution of human activities on streamflow variation in the watershed during the study period. The spatial distribution of land cover for the three dates considered, namely 1976, 1996, and 2016, indicates an increase in cultivated land of 14% during the 40 years of the study. The elasticities of precipitation and potential evapotranspiration throughout the study period, for the upstream of the watershed are 1.26 and  $-0.26$ , respectively. While in the downstream of the watershed, they are 1.35 and  $-0.35$ , respectively. This fact indicates that the response of the Merguellil Wadi is more sensitive to precipitation than to potential evapotranspiration. The direct impact of human activities on water supplies in the Merguellil watershed is responsible for more than about 55% of overall river flow change. Climate change contributes less than about 22%. Therefore, the study area is subject to intensive human impact due to social and economic development for more than 50 years. Direct human activities are the main factor in the reduction of river flow. Even more, these results show the impact of historical context in terms of anthropogenic effects.

Ultimately, the flow remains a variable and a key indicator for decision-makers to consider for its spatiotemporal variability. Therefore, it is recommended that the hydrological observation times should not be less than 30 years when analyzing flows. This allows restoring the impact of climate change and those of human activities in Tunisia. This information is essential for the sustainable management of water resources. In addition, it can give implications for analytical decisions on interpretations of the hydrological response and on planning and development both upstream and downstream of the watershed.

**Author Contributions:** Conceptualization, methodology, data collection, analysis of results, writing—original draft preparation: K.K.; methodology, writing—review and editing: S.J.; review and



editing, funding acquisition: R.B.; review and editing: K.M. All authors have read and agreed to the published version of the manuscript.

**Funding:** This research was funded by the European Union Horizon 2020 program Faster project, grant agreement N°[810812] and the PACTE program implemented by DG/ACTA and funded by AFD and FFEM.

**Institutional Review Board Statement:** Not applicable.

**Informed Consent Statement:** Not applicable.

**Data Availability Statement:** The data presented in this study are available on request from the corresponding author.

**Conflicts of Interest:** The authors declare no conflicts of interest.

## References

1. Zeng, Y.; Sarira, T.V.; Carrasco, L.R.; Chong, K.Y.; Friess, D.A.; Lee, J.S.H.; Taillardat, P.; Worthington, T.A.; Zhang, Y.; Koh, L.P. Economic and social constraints on reforestation for climate mitigation in Southeast Asia. *Nat. Clim. Chang.* **2020**, *10*, 842–844, <https://doi.org/10.1038/s41558-020-0856-3>.
2. Rakhimova, M.; Liu, T.; Bissenbayeva, S.; Mukanov, Y.; Gafforov, K.S.; Bekpergenova, Z.; Gulakhmadov, A. Assessment of the Impacts of Climate Change and Human Activities on Runoff Using Climate Elasticity Method and General Circulation Model (GCM) in the Buqtyrma River Basin, Kazakhstan. *Sustainability* **2020**, *12*, 4968, <https://doi.org/10.3390/su12124968>.
3. Piao, S.; Friedlingstein, P.; Ciais, P.; de Noblet-Ducoudré, N.; Labat, D.; Zaehle, S. Changes in climate and land use have a larger direct impact than rising CO<sub>2</sub> on global river runoff trends. *Proc. Natl. Acad. Sci. USA* **2007**, *104*, 15242–15247.
4. Wang, D.; Yu, X.; Jia, G.; Wang, H. Sensitivity analysis of runoff to climate variability and land-use changes in the Haihe Basin mountainous area of north China. *Agric. Ecosyst. Environ.* **2016**, *269*, 193–203.
5. Dey, P.; Mishra, A. Separating the impacts of climate change and human activities on streamflow: A review of methodologies and critical assumptions. *J. Hydrol.* **2017**, *548*, 278–290, <https://doi.org/10.1016/j.jhydrol.2017.03.014>.
6. Mu, X.; Wang, H.; Zhao, Y.; Liu, H.; He, G.; Li, J. Streamflow into Beijing and Its Response to Climate Change and Human Activities over the Period 1956–2016. *Water* **2020**, *12*, 622, <https://doi.org/10.3390/w12030622>.
7. Toteu, S.F.; Mahé, G.; Moritz, R.; Sracek, O.; Davies, T.C.; Ramasamy, J. Environmental, health and social legacies of mining activities in Sub-Saharan Africa. *J. Geochem. Explor.* **2020**, *209*, 106441.
8. Gai, L.; Baartman, J.E.M.; Mendoza-Carranza, M.; Wang, F.; Ritsema, C.J.; Geissen, V.A. Framework approach for unravelling the impact of multiple factors influencing flooding. *J. Flood Risk Manag.* **2018**, *11*, 111–126.
9. Cavalcante, R.B.L.; Pontes, P.R.M.; Souza-Filho, P.W.M.; de Souza, E.B. Opposite effects of climate and land use changes on the annual water balance in the Amazon arc of deforestation. *Water Resour. Res.* **2019**, *55*, 3092–3106.
10. Liu, J.; Zhang, Q.; Singh, V.P.; Shi, P. Contribution of multiple climatic variables and human activities to streamflow changes across China. *J. Hydrol.* **2017**, *545*, 145–162, <https://doi.org/10.1016/j.jhydrol.2016.12.016>, 2017.
11. Choi, W.; Nauth, K.; Choi, J.; Becker, S. Urbanization and rainfall–runoff relationships in the Milwaukee River basin. *Prof. Geogr.* **2016**, *68*, 14–25.
12. Jonoski, A.; Popescu, I.; Zhe, S.; Mu, Y.; He, Y. Analysis of Flood Storage Area Operations in Huai River Using 1D and 2D river simulation Models Coupled with Global Optimization Algorithms. *Geosciences* **2019**, *9*, 509.
13. Jebari, S.; Berndtsson, R.; Mouelhi, S.; Uvo, C.; Bahri, A. Climate Change and Transboundary Water Management in the Tunisian Mellegue Catchment. *Vatten* **2017**, *73*, 131–144.
14. Prestele, R.; Arneth, A.; Bondeau, A.; de Noblet-Ducoudré, N.; Pugh, T.A.; Sitch, S.; Stehfest, E.; Verburg, P.H. Current challenges of implementing anthropogenic land-use and land-cover change in models contributing to climate change assessments. *Earth Syst. Dyn.* **2017**, *8*, 369–386.
15. Zhang, L.; Dawes, W.R.; Walker, G.R. Response of mean annual evapotranspiration to vegetation changes at catchment scale. *Water Resour. Res.* **2001**, *37*, 701–708.
16. Guo, Y.; Li, Z.; Amo-Boateng, M.; Deng, P.; Huang, P. Quantitative assessment of the impact of climate variability and human activities on runoff changes for the upper reaches of Weihe River. *Stoch. Environ. Res. Risk Assess.* **2017**, *28*, 333–346.
17. Hu, S.; Liu, C.; Zheng, H.; Wang, Z.; Yu, J. Assessing the impacts of climate variability and human activities on streamflow in the water source area of Baiyangdian Lake. *J. Geogr. Sci.* **2012**, *22*, 895–905.
18. Budyko, M.I. *Climate and Life*, English ed.; Academic Press: New York, NY, USA, 1974; Volume 508.
19. Loehle, C.; Staehling, E. Hurricane trend detection. *Nat. Hazards* **2020**, *104*, 1345–1357, <https://doi.org/10.1007/s11069-020-04219-x>.
20. Xie, Y.Y.; Huang, Q.; Chang, J.X.; Liu, S.Y.; Wang, Y.M. Period analysis of hydrologic series through moving-window correlation analysis method. *J. Hydrol.* **2016**, *538*, 278–292.
21. Jerbi, H. Anthropisation des Processus Hydrologiques Autour de L'oued Merguellil (Tunisie Centrale): Caractérisation des Formes D'évolution et Quantification des Flux. Ph.D. Thesis, Université de Montpellier, Montpellier, France, 2018.

22. Riaux, J. Une Anthropologie “Chez” les Hydrologues. Penser la Production de Savoirs Hydrologiques à Travers la Relation Interdisciplinaire. Mémoire d’Habilitation à Diriger des Recherches. Ecole Doctorale 355. Espaces, Cultures, Sociétés. Université Aix Marseille, Marseille, France, 2019.
23. Abouabdillah, A. Hydrological Modeling in a Data-Poor Mediterranean Catchment (Merguellil, Tunisia) Assessing Scenarios of Land Management and Climate Change. Ph.D. Thesis, Tuscia University of Viterbo, Viterbo, Italy, 2009; p. 228.
24. Şen, Z. Innovative trend analysis methodology. *J. Hydrol. Eng.* **2012**, *17*, 1042–1046.
25. Şen, Z. Innovative trend significance test and applications. *Theor. Appl. Climatol.* **2015**, *127*, 1–9.
26. Li, J.; Wu, W.; Ye, X.; Jiang, H. Innovative trend analysis of main agriculture natural hazards in China during 1989–2014. *Nat. Hazards* **2019**, *95*, 677–720.
27. Tabari, H.; Taye, M.T.; Onyutha, C.; Willems, P. Decadal Analysis of River Flow Extremes Using Quantile-Based Approaches. *Water Resour. Manag.* **2017**, *31*, 3371–3387.
28. Caloiero, T. Evaluation of rainfall trends in the South Island of New Zealand through the innovative trend analysis (ITA). *Theor. Appl. Climatol.* **2019**, *139*, 493–504.
29. Alifujiang, Y.; Abuduwaili, J.; Maihemuti, B.; Emin, B.; Groll, M. Innovative Trend Analysis of Precipitation in the Lake Issyk-Kul Basin, Kyrgyzstan. *Atmosphere* **2020**, *11*, 332, <https://doi.org/10.3390/atmos11040332>.
30. Dridi, B. Impact des Aménagements CES sur la Disponibilité des Eaux de Surface Dans le Bassin Versant du Merguellil (Tunisie Centrale). Ph.D. Thesis, Univ. Louis Pasteur, Strasbourg, France, 2000; p. 194.
31. Kingumbi, A.; Besbes, M.; Bourges, J.; Garetta, P. Evaluation des transferts entre barrage et aquifères par la méthode de bilan d’une retenue en zone semi-aride. Cas d’El Haouareb en Tunisie centrale. *Revue des Sciences de l’eau* **2004**, *17*, 213–225.
32. Ben Boubaker, H.; Benzarti, Z.; Hénia, L. Les ressources en eau de la Tunisie : contraintes du climat et pression anthropique in eau et environnement, ENS Éditions, **2003**. <https://books.openedition.org/enseditions/864?lang=fr>, (accessed on October 18 2020).
33. Verner, D. La Tunisie face aux changements climatiques: Évaluation et actions pour accroître la résilience et le développement. 2013. A World Bank study; Washington, DC: World Bank. <https://openknowledge.worldbank.org/handle/10986/13114>, (accessed on October 18 2020).
34. Bouzaiane, S.; Lafforgue, A. Monographie hydrologique des oueds Zeroud et Merguellil. D.G.R.E.-ORSTOM. *Tunis* **1986**, 1058.
35. Hamza, M. *Projet de Développement Agricole du Gouvernorat de Kairouan (Ressources en eau)*; Rapp. Tech. D.G.R.E, Tunis, Tunisia, 1988; p. 90.
36. Leduc, L.; Beji, R.; Calvez, R. Les ressources en eau du barrage d’el Haouareb et des nappes adjacentes, vallée du Merguellil, Tunisie centrale. In Proceedings of the Séminaire PCSI “Gestion Intégrée de l’eau au sein d’un Bassin Versant”, Session Présentation Détaillée d’un Terrain du Sud, la Gestion du Bassin du Merguellil (Tunisie), Montpellier, France, 2 December 2003.
37. Barbery, J.; Mohdi, M. *Carte des Ressources en sols de la Tunisie (1:200,000), Feuille de Kairouan*; DCEs, Ministère de l’Agriculture: Tunis, Tunisie, 1987; p. 49.
38. Mizouri, M.; Barbery, J.; Willaine, P. *Carte des Ressources en Sols de la Tunisie (1/200.000): Nouvelle Approche Méthodologique, Feuille de Makthar*; DCEs, Ministère de l’Agriculture: Tunis, Tunisie, 1990.
39. Ouali, J. Structure et évaluation géodynamique du chaînon Nara-sidi Khalif (Tunisie centrale). *Bull. Cent. Rech. Exploration-Prod. Elf-Aquitaine* **1985**, *9*, 155–182.
40. Chadly, B. *Note sur L’évolution de la Nappe de Kairouan Après la Fermeture du Barrage d’El Haouareb*; Tunis, Tunisie, 1992; p. 24.
41. MERGUSIE. Programme de recherche (Merguellil :Ressources, Gestion et Usages Intégrés de l’Eau), vise à enrichir les connaissances sur la variabilité de la ressource en eau et les modalités de ses usages dans la vallée du Merguellil, réunit plusieurs organismes partenaires tunisiens et français : La DGRE , l’INAT, le CRDA de Kairouan et l’ENIT, les Universités de Tunis 1 et de Sfax et l’IRD. 1998–2007. [https://www.iamm.ciheam.org/en/research/projects/one\\_programme?programme=mergusie&id=51](https://www.iamm.ciheam.org/en/research/projects/one_programme?programme=mergusie&id=51), (accessed on October 02 2021).
42. DGRE. *Annuaire Hydrologique de la Tunisie*; Publication de la Direction Générale des Ressources en Eau: Tunisia, 2017.
43. INM. *Annuaire météorologique de la Tunisie*; Publication de l’Institut National de la Météorologie: Tunis, Tunisia, 2020.
44. Roudier, P.; Mahé, G. Calcul des pluies et débits classés sur le bassin du Bani (Mali): Une approche de la vulnérabilité des ouvrages et de la population depuis la sécheresse. *Hydrol. Sci. J.* **2010**, *55*, 351–363.
45. Barros, A. P. Orographic Precipitation, Freshwater Resources, and Climate Vulnerabilities in Mountainous Regions. *Climat. Vulnerab.* **2013**, *57*–78, <https://doi.org/10.1016/b978-0-12-384703-4.00504-9>.
46. Mu, Q.; Zhao, M.; Running, S.W. Improvements to a MODIS global terrestrial evapotranspiration algorithm. *Remote Sens. Environ.* **2011**, *115*, 1781–1800.
47. Gao, P.; Li, P.; Zhao, B.; Xu, R.; Zhao, G.; Sun, W.; Mu, X. Use of double mass curves in hydrologic benefit evaluations. *Hydrol. Process.* **2017**, *31*, 4639–4646.
48. Owolabi, S.T.; Madi, K.; Kalumba, A.M.; Alemaw, B.F. Assessment of recession flow variability and the surficial lithology impact: A case study of Buffalo River catchment, Eastern Cape, South Africa. *Environ. Earth Sci.* **2020**, *79*, 1–19, <https://doi.org/10.1007/s12665-020-08925-4>.
49. Choate, M.; Steinwand, D.; Rengarajan, R. *Multispectral Scanner (MSS) Geometric Algorithm Description Document; USGS Landsat Project Documentation*; LS-IAS: Delhi, India, 2012; Volume 6.

50. Engebretson, C. *Landsat Thematic Mapper (TM) Level 1 DFCB*; USGS Landsat Project Documentation; 2018. [https://prd-wret.s3.us-west-2.amazonaws.com/assets/palladium/production/atoms/files/LSDS-284\\_Landsat4-5TM-Level1DFC-B-v10.pdf](https://prd-wret.s3.us-west-2.amazonaws.com/assets/palladium/production/atoms/files/LSDS-284_Landsat4-5TM-Level1DFC-B-v10.pdf), (accessed on October 02 2021).
51. Serinaldi, F.; Chebana, F.; Kilsby, C.G. Dissecting innovative trend analysis. *Stoch. Environ. Res. Risk Assess.* **2020**, *34*, 733–754, <https://doi.org/10.1007/s00477-020-01797-x>.
52. Wang, W.; Zhu, Y.; Liu, B.; Chen, Y.; Zhao, X. Innovative Variance Corrected Sen's Trend Test on Persistent Hydrometeorological Data. *Water* **2019**, *11*, 2119, <https://doi.org/10.3390/w11102119>.
53. Alashan, S. Comparison of Sub-Series with Different Lengths Using Şen-Innovative Trend Analysis. *Res. Sq.* **2021**, [https://assets.researchsquare.com/files/rs-554023/v1\\_covered.pdf?c=1631869036](https://assets.researchsquare.com/files/rs-554023/v1_covered.pdf?c=1631869036), (accessed on October 02 2021).
54. Zheng, H.; Zhang, L.; Zhu, R.; Liu, C.; Sato, Y.; Fukushima, Y. Responses of streamflow to climate and land surface change in the headwaters of the Yellow River Basin. *Water Resour. Res.* **2009**, *45*, <https://doi.org/10.1029/2007WR00666>.
55. Sankarasubramanian, A.; Vogel, R.M.; Limbrunner, J.F. Climate elasticity of streamflow in the United States. *Water Resour. Res.* **2001**, *37*, 1771–1781.
56. Fu, G.; Charles, S.P.; Chiew, F.H.S. A two-parameter climate elasticity of streamflow index to assess climate change effects on annual streamflow. *Water Resour. Res.* **2007**, *43*, <https://doi.org/10.1029/2007WR005890>.
57. Sun, Y.; Tian, F.; Yang, L.; Hu, H. Exploring the spatial variability of contributions from climate variation and change in catchment properties to streamflow decrease in a mesoscale basin by three different methods. *J. Hydrol.* **2014**, *508*, 170–180.
58. Xing, W.; Wang, W.; Zou, S.; Deng, C. Projection of future runoff change using climate elasticity method derived from Budyko framework in major basins across China. *Glob. Planet. Chang.* **2018**, *162*, 120–135.
59. Kazemi, H.; Hashemi, H.; Maghsood, F.F.; Hosseini, S.H.; Sarukkalige, R.; Jamali, S.; Berndtsson, R. Assessment of streamflow decrease due to climate vs. human influence in a semiarid area. *Hydrol. Earth Syst. Sci. Discuss.* **2020**, <https://hess.copernicus.org/preprints/hess-2019-618/>, (accessed on October 02 2021).
60. Thornthwaite, C.W. An approach toward a rational classification of climate. *Geogr. Rev.* **1948**, *38*, 55–94, <https://doi.org/10.2307/210739>.
61. Lu, J.; Sun, G.; Nulty, M.C.; Steven, G.; Amatya, D. A comparison of six potential evapotranspiration methods for regional use in the Southeastern United States. *J. Am. Water Resour. Assoc.* **2005**, *41*, 621–633.
62. Wang, W.; Shao, Q.; Yang, T.; Peng, S.; Xing, W.; Sun, F.; Luo, Y. Quantitative assessment of the impact of climate variability and human activities on runoff changes: A case study in four catchments of the Haihe River basin, China. *Hydrol. Process.* **2012**, *27*, 1158–1174.
63. Rouse, J.W.; Haas, R.H.; Schell, J.A.; Deering, D.W. *Monitoring the Vernal Advancement and Retrogradation (Green Wave Effect) of Natural Vegetation*; Final Report. RSC 1978-1; Remote Sensing Center, Texas A&M Univ., College Station, NASA/GSFC, Greenbelt, 1974.
64. Kingumbi, A.; Bargaoui, Z.; Hubert, P. Investigation of the rainfall variability in central Tunisia. *Hydrol. Sci. J.* **2005**, *50*, 493–508.
65. Sakiss, N.; Ennabli, N.; Slimani, M.S.; Baccour, H. La pluviométrie en Tunisie a-t-elle changé depuis 2000 ans? Tunis: Institut National de la Météorologie & Institut National Agronomique de Tunisie. 1994. [http://www.credif.org.tn/PORT/doc/SYRACUSE/19780/la-pluviometrie-en-tunisie-a-t-elle-change-depuis-2000-ans-recherche-de-tendances-et-de-cycles-dans-\\_lg=fr-FR](http://www.credif.org.tn/PORT/doc/SYRACUSE/19780/la-pluviometrie-en-tunisie-a-t-elle-change-depuis-2000-ans-recherche-de-tendances-et-de-cycles-dans-_lg=fr-FR), (accessed on October 02 2021).
66. Benzarti, Z.; Habaieb, H. Étude de la persistance de la sécheresse en Tunisie par utilisation des chaînes de Markov (1909–1996). *Sécheresse* **2001**, *12*, 215–220.
67. Slimani, M.; Cudennec, C.; Feki, H. Structure du gradient pluviométrique de la transition Méditerranée-Sahara en Tunisie: Déterminants géographiques et saisonnalité. *Hydrol. Sci. J.* **2007**, *52*, 1088–1102.
68. Proaño, D. Bilan Offres-Demandes sur le Bassin Versant du Merguellil à L'aide de la Plateforme WEAP. MSc Thesis, Université de Montpellier 2, Montpellier, France, 2012.
69. Andréassian, V.; Coron, L.; Lerat, J.; Le Moine, N. Climate elasticity of streamflow revisited—An elasticity index based on long-term hydrometeorological records. *Hydrol. Earth Syst. Sci.* **2016**, *20*, 4503–4524, <https://doi.org/10.5194/hess-20-4503-2016>.
70. Vogel, R.M.; Wilson, I.; Daly, C. Regional Regression Models of Annual Streamflow for the United States. *J. Irrig. Drain. Eng.* **1999**, *125*, 148–157, [https://doi.org/10.1061/\(asce\)0733-9437\(1999\)125:3\(148\)](https://doi.org/10.1061/(asce)0733-9437(1999)125:3(148)).
71. Lee, C.H.; Yeh, H.F. Impact of Climate Change and Human Activities on Streamflow Variations Based on the Budyko framework. *Water* **2019**, *11*, 2001, <https://doi.org/10.3390/w11102001>.
72. IPCC. *Climate Change: Synthesis Report. Contribution of Working Groups I, II and III to the Fifth Assessment Report of the Intergovernmental Panel on Climate Change*; IPCC: Geneva, Switzerland, 2014. <https://www.ipcc.ch/report/ar5/syr>.
73. Tsai, Y. The multivariate climatic and anthropogenic elasticity of streamflow in the Eastern United States. *J. Hydrol. Reg. Stud.* **2017**, *9*, 199–215, <https://doi.org/10.1016/j.ejrh.2016.12.078>.
74. FAO (Food and Agriculture Organization). *The State of the World's Forests 2020. Forests, Biodiversity and People*; FAO: Rome, Italy, 2020, <https://doi.org/10.4060/ca8642en>.
75. PIF. *Programme d'Investissement Forestier. Plan d'Investissement*; Tunis, 30 Septembre 2016. [https://www.climateinvestmentfunds.org/sites/default/files/meeting-documents/fip\\_tunisia\\_joint\\_mission\\_aide\\_memoire\\_june\\_20-24\\_2016french.pdf](https://www.climateinvestmentfunds.org/sites/default/files/meeting-documents/fip_tunisia_joint_mission_aide_memoire_june_20-24_2016french.pdf), (accessed on October 02 2021).

- 
76. GIZ. *Etude de la Filière des Céréales Dans le Gouvernorat du Kairouan-Projet « Promotion de L'agriculture Durable et du Développement rural- Filière Céréales dans le Gouvernorat de Kairouan. Deutsche Gesellschaft für Internationale Zusammenarbeit (GIZ) GmbH. Rapport Final; GIZ: Bonn, Germany, 2014; p. 45.*
  77. Riaux, J.; Massuel, M. Construire un regard sociohydrologique (2). Le terrain en commun, générateur de convergences scientifiques. *Nat. Sci. Soc.* **2014**, *22*, 329–333.
  78. Scanlon, B.R.; Keese, K.E.; Flint, A.L.; Flint, L.E.; Gaye, C.B.; Edmunds, W.M.; Simmers, I. Global synthesis of groundwater recharge in semiarid and arid regions. *Hydrol. Process.* **2006**, *20*, 3335–3370.
  79. Salem, M.A. Approches Hydrodynamique et Géochimique de la Recharge de la Nappe du Trarza, Sudoued de la Mauritanie., 2012; p. 133.
  80. Cudennec, C.; Leduc, C.; Koutsoyiannis, D. Dryland hydrology in Mediterranean regions-a review. *Hydrol. Sci. J.* **2007**, *52*, 1077–1087.
  81. Kingumbi, A.; Bargaoui, Z.; Ledoux, E.; Besbes, M.; Hubert, P. Modélisation hydrologique stochastique d'un bassin affecté par des changements d'occupation : Cas du Merguellil en Tunisie centrale. *Hydrol. Sci. J.* **2007**, *52*, 1232–1252.
  82. Ogilvie, A.; Le Goulven, P.; Leduc, C.; Calvez, R.; Mulliga, M. Réponse hydrologique d'un bass in semi-aride aux événements pluviométriques et aménagements de versant (bassin du Merguellil, Tunisie centrale). *Hydrol. Sci. J.* **2014**, *61*, 441–453.
  83. Lacombe, G.; Cappelaere, B.; Leduc, C. Hydrological impact of water and soil conservation works in the Merguellil catchment of central Tunisia. *J. Hydrol.* **2008**, *359*, 210–224.